Application of the generalized scattering amplitude in quantum potential scatterings

R. T. Ling
4715 Lasheart Drive, La Canada, California 91011-2128
(Received 23 December 1993; revised manuscript received 22 February 1994)

The concept of a generalized scattering amplitude is introduced and applied to quantum potential scatterings. After an outgoing spherical wave is factored out from a wave function, the remaining wave envelope is defined as the generalized scattering amplitude. The transformed Schrödinger equation, in terms of the generalized scattering amplitude, can be solved numerically by using a finite-difference method over the entire scattering domain. Example problems of scatterings by a spherical potential well and the (e^-,H) static field interaction potential are solved to validate the theoretical formulation and numerical method. The far-field solutions for the ordinary scattering amplitude and differential cross section agree very well with those obtained from the partial-wave analysis. The radial profiles of the generalized scattering amplitude and particle density function over the entire scattering region are also presented, and their properties are discussed. These results demonstrate that the method can be used to yield a complete and accurate solution to scattering problems involving arbitrary interaction potentials.

PACS number(s): 03.80.+r, 03.65.Nk, 11.55.−m, 02.70.Bf

I. INTRODUCTION

Angular momentum is a fundamental concept in quantum mechanics. The numerical solution of the Schrödinger equation in potential scattering problems, particularly in the low-energy regime, is usually obtained through a partial-wave analysis. Each partial wave in the partial-wave analysis is tied directly to the orbital angular momentum of the scattered particle. Even when the scattering problem is formulated as an integral equation for the wave function, the Green's function is often expanded as a sum of partial-wave Green's functions for numerical solutions.

Though the partial-wave analysis has the advantage of reducing a three-dimensional numerical problem to a set of three one-dimensional problems, the radial component of the reduced partial-wave Schrödinger equation is still difficult to solve due to the oscillatory behavior of the solution and the infinite radial range of the scattering process. Only in some special cases, such as in the scattering by a spherical potential well, can analytical and closed form solutions be obtained. Other difficulties for the partial-wave analysis include a slow convergence in the high-energy regime when many partial waves are required for convergence; moreover, each partial wave has its own differential equation to be solved.

In principle, instead of the partial-wave analysis, the governing three-dimensional Schrödinger equation can be solved directly to yield the same solution. This has been recognized for some time [1]. Sullivan and Temkin applied a finite-difference method to solve a partial differential equation in electron scatterings by atomic and molecular systems. The main obstacle to this direct solution of partial differential equation approach is the infinite domain of the scattering region and the oscillatory nature of the wave function. In other words, the major difficulty lies in the enforcement of the far-field asymptotic condition. In the partial-wave analysis, this difficulty is avoided by choosing basis set functions that automatically satisfy the far-field asymptotic condition. In direct solution of partial differential equations, this difficulty is usually dealt with by truncating the computational domain to a finite domain near the scattering center. But since the outer computational boundary is not at the far field, some sort of approximate boundary conditions needs to be used. Several approximating schemes, so-called absorbing boundary conditions, have been proposed for atomic scatterings [2], classical acoustic, and electromagnetic scatterings [3].

In this paper, the concept of the generalized scattering amplitude is introduced to overcome this difficulty and to avoid using absorbing boundary conditions. The formulation of potential scattering problems in terms of the generalized scattering amplitude allows the transformed Schrödinger equation to be solved exactly over the entire scattering domain without truncation. In this approach, the potential scattering problem is treated as a boundary value problem. The transformed Schrödinger equation is the governing equation. It couples with the far-field asymptotic condition in terms of the generalized scattering amplitude to yield the solution to the scattering problem.

The concept of the generalized scattering amplitude [4,5] was first introduced in solving analogous classical scatterings of acoustic and electromagnetic waves. The similarity between quantum and classical scatterings can be evidenced by the fact that the whole mathematical machinery of the partial-wave analysis was developed and applied [6] to scatterings of acoustic and electromagnetic waves by spheres in the nineteenth century, well before the founding of quantum mechanics. The common thread linking quantum potential scattering with classical scatterings is the Helmholtz equation in the form of the time-independent Schrödinger equation or the reduced wave equation governing these physically similar phenomena.

The key to the concept of the generalized scattering amplitude is the recognition that the outgoing spherical wave modulates the scattered wave. By factoring out the outgoing spherical wave in the scattered wave part of the wave function, the encompassing wave envelope, defined as the generalized scattering amplitude, is not oscillatory in the radial direction. It varies smoothly, though rapidly, near the scattering center, and approaches the ordinary scattering amplitude asymptotically in the far field. Because of this behavior, by using stretching coordinates in the radial direction, one needs only a finite number of radial grid points to resolve the radial variation of the generalized scattering amplitude along the infinite radial range. The oscillatory wave function can be reconstructed by first recombining the generalized scattering amplitude with the outgoing spherical wave and then with the incident plane wave.

II. THEORETICAL FORMULATION

In this section, a quantum potential scattering is formulated as a boundary value problem in terms of the generalized scattering amplitude. The problem under consideration is that of an incident beam of particles of energy E scattered by a potential of the form $V(\mathbf{r})$. The scattering process is governed by the time-independent Schrödinger equation,

$$-\frac{\hbar^2}{2m}\nabla^2\Psi(\mathbf{r})+V(\mathbf{r})\Psi(\mathbf{r})=E\Psi(\mathbf{r}) , \tag{1}$$

or

$$[\nabla^2+k_0^2-U(\mathbf{r})]\Psi(\mathbf{r})=0 , \tag{2}$$

with $E=\hbar^2k_0^2/2m$ and $U(\mathbf{r})=(2m/\hbar^2)V(\mathbf{r})$. The wave function $\Psi(\mathbf{r})$ is regular at the scattering center,

$$\lim_{r\to 0}\Psi(\mathbf{r})=\text{finite} . \tag{3}$$

With the incident beam particles represented by a plane wave, the wave function assumes the asymptotic form

$$\lim_{r\to\infty}\Psi(\mathbf{r})=e^{i\mathbf{k}_0\cdot\mathbf{r}}+\frac{e^{ik_0r}}{k_0r}f(\theta,\phi) , \tag{4}$$

where the incident wave vector $\mathbf{k}_0$ is assumed to lie in the positive z axis.

The potential scattering problem is thus defined by the governing partial differential equation, Eq. (2), and boundary conditions, Eqs. (3) and (4), over the entire physical space. This constitutes a boundary value problem. The asymptotic form of the wave function in Eq. (4) is valid only in the far-field limit, and the far-field scattering amplitude $f(\theta,\phi)$ is independent of the radial distance variable r. The range of validity of Eq. (4) can be extended inward by introducing the radial distance dependence into f, so that a new unknown function $f_0(r,\theta,\phi)$, defined as the *generalized scattering amplitude,* can be substituted for $f(\theta,\phi)$ in Eq. (4). The new functional form,

$$\Psi_0(\mathbf{r})=e^{i\mathbf{k}_0\cdot\mathbf{r}}+\frac{e^{ik_0r}}{k_0r}f_0(r,\theta,\phi) \quad \text{for } r\geq a , \tag{5}$$

is valid not only in the far field, but also in the exterior scattering region outside a certain range parameter a. The range parameter specifies the range of the potential outside which the potential is small and diminishing. The choice of values for a is arbitrary. For a square well potential, it can be conveniently chosen so that $r=a$ coincides with the boundary of the well. In the remaining spatial domain, defined by $r\leq a$, the wave function is assumed to have the form

$$\Psi_1(\mathbf{r})=\frac{e^{ik_0r}}{k_0r}f_1(r,\theta,\phi) \quad \text{for } r\leq a , \tag{6}$$

where f_1 is the generalized scattering amplitude in the interior scattering region. The absence of the plane wave in the wave function $\Psi_1(\mathbf{r})$ in the interior scattering region is sometimes referred to as due to the extinction theorem [7]. In the scattering of electromagnetic waves by a dielectric sphere, which is physically similar to the scattering of particles by a spherical potential barrier, the extinction theorem states that the distribution of the induced internal field inside the sphere is such that the incident field is exactly cancelled out everywhere inside the dielectric sphere, i.e., the plane wave cannot penetrate the sphere.

To maintain a regular solution at the scattering center, the generalized scattering amplitude in the interior region vanishes there, i.e.,

$$f_1(r,\theta,\phi)=0 \quad \text{at } r=0 . \tag{7}$$

The choice of Eq. (5) as the functional form of the wave function in the exterior scattering region leads to a very simple outer boundary condition. In terms of the generalized scattering amplitude, the far-field asymptotic condition becomes

$$\lim_{r\to\infty}\frac{\partial f_0}{\partial r}(r,\theta,\phi)=0 , \tag{8}$$

indicating the independence of the generalized scattering amplitude on the radial distance variable in the far field. The vanishing of the first derivative with respect to the radial distance variable also is manifest in flat radial profiles of the generalized scattering amplitude in the far field, as will be shown in Sec. IV.

It is interesting to note that in treating classical acoustic and electromagnetic scatterings, the far-field asymptotic condition is called the Sommerfeld radiation condition. Rather than expressing the field quantities in their asymptotic forms as in Eq. (4), the far-field boundary condition [8] is instead given by

$$\lim_{r\to\infty}(\mathbf{r}\times\nabla\times\mathbf{E}^s+ikr\mathbf{E}^s)=\mathbf{0} , \tag{9}$$

for electromagnetic scattering where $\mathbf{E}^s$ is the scattered electric field and by

$$\lim_{r\to\infty} r\left(\frac{\partial}{\partial r}V^s-ikV^s\right)=0 , \tag{10}$$

for acoustic scattering where V^s is the scattered wave part of the acoustic pressure. When V^s and the angular components of $\mathbf{E}^s$ are factored into outgoing spherical

waves and the generalized scattering amplitude as in Eq. (5), and their expressions substituted in Eqs. (9) and (10), the Sommerfeld radiation condition reduces to a form identical to Eq. (8) for the corresponding electromagnetic and acoustic generalized scattering amplitudes [4,5].

For simplicity and without loss of generality, the interaction potential will be assumed to be spherically symmetric, $U(\mathbf{r})=U(r)$. The wave function becomes independent of the azimuthal angle ϕ. Since the plane wave satisfies the free space wave equation, substitution of Eq. (5) in the Schrödinger equation, Eq. (2), results in the transformed Schrödinger equation,

$$\frac{\partial^2 f_0}{\partial r^2}+2ik_0\frac{\partial f_0}{\partial r}+\frac{\cot\theta}{r^2}\frac{\partial f_0}{\partial\theta}+\frac{1}{r^2}\frac{\partial^2 f_0}{\partial\theta^2}-U(r)f_0(r,\theta)=(k_0r)U(r)e^{ik_0r(\cos\theta-1)}, \quad (11)$$

for the exterior region, $r\geq a$. The potential is assumed to vanish faster than the Coulomb potential in the exterior scattering region, so that the right-hand side of Eq. (11) vanishes in the far field. Similar substitution of Eq. (6) in Eq. (2) results in the transformed Schrödinger equation

$$\frac{\partial^2 f_1}{\partial r^2}+2ik_0\frac{\partial f_1}{\partial r}+\frac{\cot\theta}{r^2}\frac{\partial f_1}{\partial\theta}+\frac{1}{r^2}\frac{\partial^2 f_1}{\partial\theta^2}-U(r)f_1(r,\theta)=0, \quad (12)$$

for the interior region, $r\leq a$.

Along the forward and backward scattering directions, at $\theta=0$ and π, respectively, it can be shown [5] that

$$\cot(\theta)\frac{\partial f_0}{\partial\theta}=\frac{\partial^2 f_0}{\partial\theta^2} \quad \text{and} \quad \cot(\theta)\frac{\partial f_1}{\partial\theta}=\frac{\partial^2 f_1}{\partial\theta^2}$$

due to the symmetry property of the transformed Schrödinger equation and boundary conditions under the transformation $\theta\rightarrow-\theta$ at $\theta=0$ and π. Therefore the transformed Schrödinger equation assumes the particular forms

$$\frac{\partial^2 f_0}{\partial r^2}+2ik_0\frac{\partial f_0}{\partial r}+\frac{2}{r^2}\frac{\partial^2 f_0}{\partial\theta^2}-U(r)f_0(r,\theta)=(k_0r)U(r)e^{ik_0r(\cos\theta-1)}, \quad r\geq a \quad (11')$$

$$\frac{\partial^2 f_1}{\partial r^2}+2ik_0\frac{\partial f_1}{\partial r}+\frac{2}{r^2}\frac{\partial^2 f_1}{\partial\theta^2}-U(r)f_1(r,\theta)=0, \quad r\leq a \quad (12')$$

at $\theta=0$ and π. No singularity exists in the governing equations at any θ angle.

At the boundary between the interior and the exterior scattering regions, $r=a$, the wave functions and their first-order radial derivatives are required to be continuous across the boundary,

$$\Psi_1(r,\theta)=\Psi_0(r,\theta) \quad \text{at } r=a \quad (13)$$

and

$$\frac{\partial}{\partial r}\Psi_1(r,\theta)=\frac{\partial}{\partial r}\Psi_0(r,\theta) \quad \text{at } r=a\ . \quad (14)$$

These two relationships can be transformed into corresponding relationships between f_0 and f_1 by using Eqs. (5) and (6). The potential scattering process now becomes a boundary value problem defined by the governing equations, Eqs. (11), (12), (11'), and (12'), and boundary conditions, Eqs. (7), (8), (13), and (14).

Being defined as the wave envelope of the scattered wave in the exterior scattering region and dictated by the far-field boundary condition, the exterior region generalized scattering amplitude f_0 is expected to be nonoscillatory in the radial direction. Its radial profiles should reach certain plateaus in the far field. These expectations are borne out in previous applications in classical acoustic and electromagnetic scatterings. This is also shown to be the case in quantum potential scattering to be discussed below.

Since the generalized scattering amplitude approaches the ordinary scattering amplitude in the far field, the differential cross section is given by

$$\frac{d\sigma(\theta)}{d\Omega}=\frac{1}{k_0^2}|f_0(\infty,\theta)|^2\ . \quad (15)$$

The optical theorem that can be used as a numerical check is still valid and is given by

$$\sigma_t=\int\frac{d\sigma}{d\Omega}d\Omega=\frac{4\pi}{k_0^2}\mathrm{Im}f_0(\infty,0)\ , \quad (16)$$

where the total cross section σ_t can be obtained either by integrating the differential cross sections over all scattering angles or by multiplying the imaginary part of the forward scattering amplitude with a constant.

III. NUMERICAL METHODS

The boundary value problem for the potential scattering process as defined in Sec. II can be solved by a finite-difference method. The radially nonoscillatory, smoothly varying behavior of the generalized scattering amplitude f_0 in the exterior region allows one to make suitable coordinate transformations to map the infinite physical domain outside the $r=a$ boundary onto a finite computational domain. Tangent and inverse hyperbolic tangent functions are examples of such coordinate transformations. The finite-difference discretization of the governing partial differential equation and boundary conditions converts the boundary value problem into a large simultaneous algebraic equation that can be written in a banded matrix equation form. This banded matrix equation can then be solved by conventional direct matrix inversion methods. Examples and details of this procedure are given in Refs. [4,5].

For quantum potential scattering, in addition to the infinite exterior scattering region, there is the interior scattering region to contend with. The scattering in the interior region is dominated by the interaction potential. The generalized scattering amplitude can have radial oscillations in this region. Fortunately, the interior region is of finite size, limited by the $r=a$ boundary. A sufficiently dense grid can be provided to resolve the radial oscillation if necessary. The matrix inversion method can be extended to include the interior region with the in-

corporation of continuity relationships for the wave funtion and its radial slope, Eqs. (13) and (14), at the regional boundary, $r=a$. The numerical results presented in this paper are obtained by such a direct matrix inversion method.

In the following, two possible alternatives to the direct matrix inversion method are suggested and described. These two alternatives have not been applied to quantum potential scattering, but they have been successfully demonstrated in classical acoustic and electromagnetic scatterings which have similar numerical problems. In classical scatterings, though the banded matrix derived from finite-difference discretization of Helmholtz equation is sparse, major difficulties often arise in using the direct matrix inversion method due to large computer memory requirement and round-off error when the matrix becomes large in the high-energy and three-dimensional scattering regimes. An alternative to the direct matrix inversion method is the iterative method. However, due to the nonpositive definite property [9] of matrices resulting from the Helmholtz equation, many iterative methods are shown to give divergent results. Only the normal-equation-type methods such as the conjugate gradient method [10] can handle the nonpositive definite matrices. Other disadvantages of iterative matrix solvers include slow convergence, particularly when the matrix's condition number is large. Several preconditioning schemes [11] to speed up the convergence have been proposed.

Another alternative to the matrix inversion method of solving the time-independent boundary value problem is to transform the problem into a time-dependent initial value problem. The transformation is accomplished by introducing a time dependence into the generalized scattering amplitude for classical scatterings and starting with the wave equation instead of the Helmholtz equation to derive a time-dependent partial differential equation for the new time-dependent generalized scattering amplitude. This procedure transforms the original elliptic boundary value problem involving only spatial coordinates into a hyperbolic initial value problem involving both spatial and temporal coordinates. The time-harmonic steady state solution is obtained when the time-stepping process reaches convergence. An example is given in Ref. [12] where a time-marching scheme is used to reproduce the results for the classical acoustic and electromagnetic scatterings by infinitely long circular cylinders and spheres that were previously obtained using the direct matrix inversion method. Recently this time-marching method was generalized and applied to the three-dimensional acoustic scattering by an almond-shaped obstacle [13]. The time-dependent iterative method is very efficient in computer memory storage.

As indicated above, these two alternatives to the direct matrix inversion method have not been applied to quantum potential scatterings. For quantum scattering involving arbitrary interaction potentials, the inclusion of the interior scattering region and additional constraints on the wave function, Eqs. (13) and (14), may affect the convergence and numerical stability of these two alternative numerical schemes.

IV. RESULTS AND DISCUSSION

The theoretical formulation presented in Sec. II and the finite-difference approach using the direct matrix inversion method described in Sec. III are applied to two quantum potential scattering problems. For convenience, atomic units are used throughout the computations. The unit of length in this system is the Bohr radius a_0.

A. Square well potential scattering problem

In this problem, the incident particles are scattered by an attractive square well potential of well depth $U(r)=-10$ and well radius $r_0=1$. The incident particles are assumed to have an incident wave number k_0 equal to 3.1 so that their de Broglie wavelengths are roughly equal to the diameter of the well. The range parameter a is set to unity so that the boundary between the interior and exterior regions coincides with the well's outer boundary. Representative results based on the solutions of interior and exterior region generalized scattering amplitudes f_0 and f_1 are given. The radial profiles of the generalized scattering amplitudes in the forward ($\theta=0$), vertical ($\theta=\pi/2$), and backward ($\theta=\pi$) scattering directions are shown in Figs. 1 and 2. Perspective three-dimensional surface plots of the interior and exterior region generalized scattering amplitudes as functions of radial distance and scattering angle are shown in Figs. 3–6.

The radial profiles of the exterior region generalized scattering amplitude outside the potential well as shown in Figs. 2, 5, and 6 are similar to those of classical acoustic and electromagnetic scatterings [4,5]. They change smoothly and rapidly near the well boundary and approach some asymptotic plateaus in the far field without oscillations. The characteristics of these profiles allow the numerical solution to be carried out with larger and larger grid spacings in the far field without resorting to truncation of the computational domain and without using approximate absorbing boundary conditions. Some

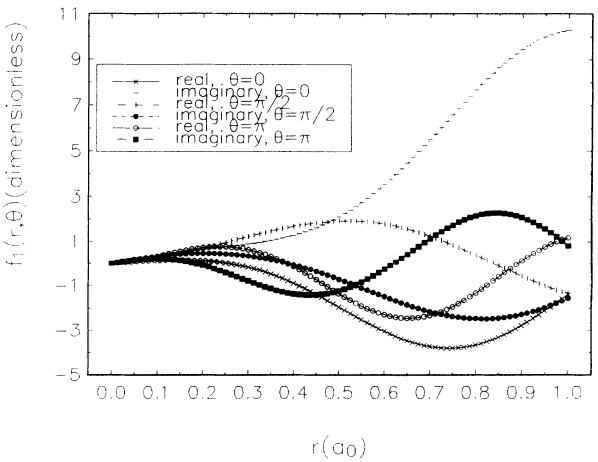

FIG. 1. Radial profiles of the generalized scattering amplitude $f_1(r,\theta)$ in the interior scattering region. Square well potential scattering, $k_0=3.1$, $U=-10$. The radial distance r is in units of a_0, the atomic unit for length.

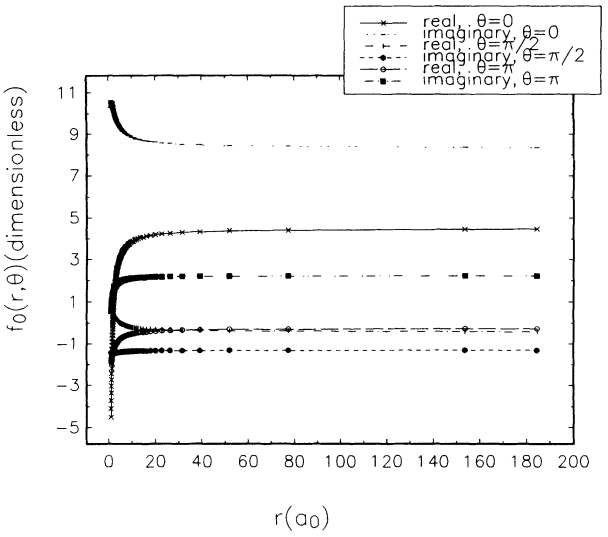

FIG. 2. Radial profiles of the generalized scattering amplitude $f_0(r,\theta)$ in the exterior scattering region. Square well potential scattering, $k_0=3.1$, $U=-10$. The radial distance r is in units of a_0, the atomic unit for length.

researchers [14] divide the whole physical space in a scattering process into *inner regia* and *outer regia* in order to separate the region of rapid changes from the asymptotic plateau area. The radial profiles of the generalized scattering amplitude in the exterior region shown here offer a clear view of the division.

The far-field values of the exterior region generalized scattering amplitude as a function of scattering angle are shown in Fig. 7. The differences between the present computation and the partial-wave analysis are less than 0.4% for all angles. The two solutions are indistinguishable in the graph shown in Fig. 7. Twelve partial waves are sufficient for convergence at $k_0=3.1$. The generalized scattering amplitude computation uses a grid network of 180×65, with 80 grid points uniformly distributed in the radial direction in the interior scattering region

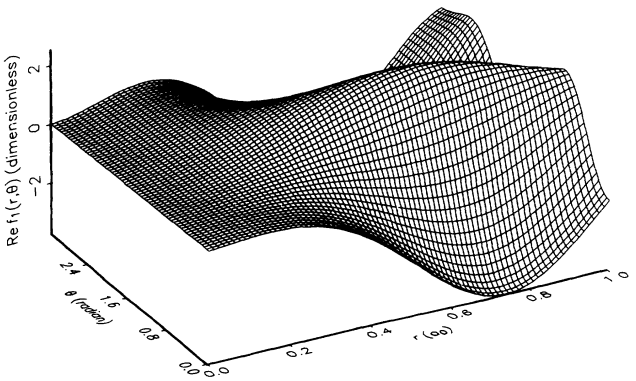

FIG. 3. Perspective three-dimensional (3D) surface plot of the real part of the generalized scattering amplitudes in the interior scattering region. Square well potential scattering, $k_0=3.1$, $U=-10$. The radial distance r is in units of a_0, the atomic unit for length. The scattering angle is denoted by θ.

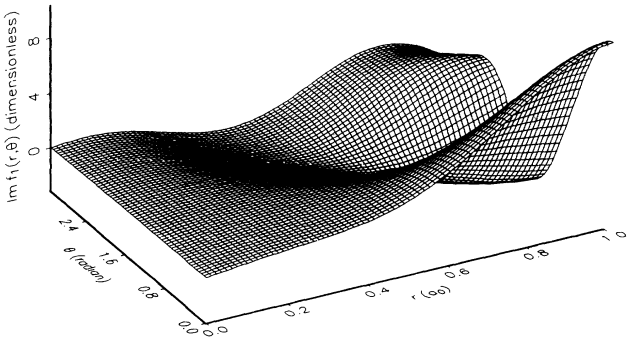

FIG. 4. Perspective 3D surface plot of the imaginary part of the generalized scattering amplitudes in the interior scattering region. Square well potential scattering, $k_0=3.1$, $U=-10$. The radial distance r is in units of a_0, the atomic unit for length. The scattering angle is denoted by θ.

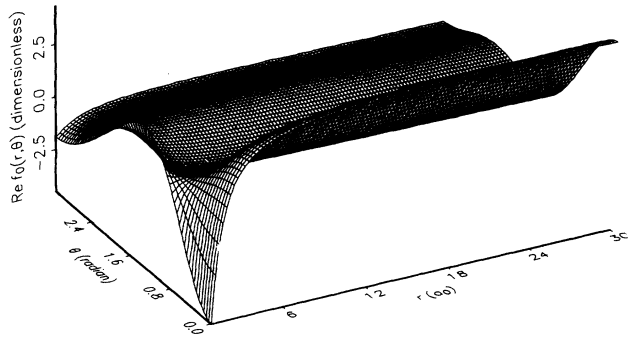

FIG. 5. Perspective 3D surface plot of the real part of the generalized scattering amplitudes in the exterior scattering region. Square well potential scattering, $k_0=3.1$, $U=-10$. The radial distance r is in units of a_0, the atomic unit for length. The scattering angle is denoted by θ.

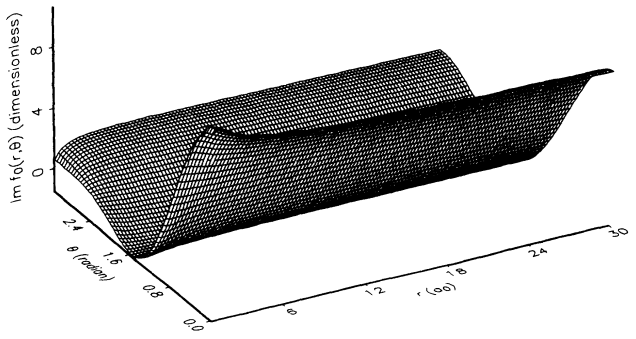

FIG. 6. Perspective 3D surface plot of the imaginary part of the generalized scattering amplitudes in the exterior scattering region. Square well potential scattering, $k_0=3.1$, $U=-10$. The radial distance r is in units of a_0, the atomic unit for length. The scattering angle is denoted by θ.

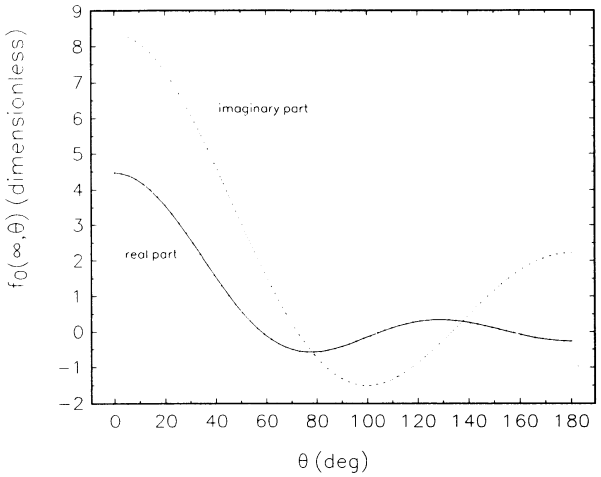

FIG. 7. Angular distribution of far-field scattering amplitude. Square well potential scattering, $k_0=3.1$, $U=-10$. The scattering angle is denoted by θ.

$(0\le r\le 1)$, 100 grid points distributed tangentially along the radial direction in the exterior scattering region $(1\le r\le\infty)$, and 65 grid points distributed uniformly over the range of scattering angles $(0\le\theta\le\pi)$. The distribution of the differential cross section, as a function of scattering angle and computed using Eq. (15), is shown in Fig. 8. Again the generalized scattering amplitude method yields values nearly identical to the partial-wave analysis. The difference between the two solutions is too small to be distinguished in Fig. 8. The total cross section σ_t obtained from the integration of differential cross sections is equal to 10.864 while it is equal to 10.922 from the optical theorem, Eq. (16). The exact partial-wave analysis yields 10.863 for the total cross section.

The computational results presented for the 180×65 grid network were obtained from a run on a Cray Y-MP C90 machine that took 72 seconds of single processor CPU time and 24 megawords of core memory. The computer code was neither vectorized nor optimized. The 180×65 grid was deemed sufficient when doubling the number of grid points in either r or θ direction, i.e., with a 360×65 or a 180×129 grid, yielded identical results in five digits. The phase shift computation using analytical expressions of the partial-wave analysis, which provides the far-field scattering amplitudes and differential cross sections for comparison with the present generalized scattering amplitude computation (Figs. 7 and 8), can be performed in a fraction of a second on the Cray machine. However, it is understood that the phase shift results provide only the wave function solution in the far field, in contrast to the global wave function solution afforded by the generalized scattering amplitude method. No attempt was made in using the analytical expressions of the partial-wave analysis to compute the near-field wave function in the square well potential scattering. Therefore no computational efficiency comparison is available. For arbitrary interaction potentials other than the square well potential, no closed form analytical solutions are available for the phase shift and radial part of the wave function in the partial-wave analysis. The computation would involve solving a series of orbital angular-momentum-dependent ordinary differential equations. No specific comments on the numerical efficiency in this type of computation can be made.

Figure 9 shows the radial profiles of the particle density function, $\rho(r,\theta)$, defined as $|\Psi(r,\theta)|^2$, in the forward, vertical, and backward scattering directions. Figure 10 is a perspective three-dimensional plot of the particle density function for all scattering angles and for radial distances up to 20 Bohr radii. In the interior region, the particle density function is given by $\rho(r,\theta)=[(\mathrm{Re}f_1)^2+(\mathrm{Im}f_1)^2]/(k_0^2r^2)$, for all angles. In the exterior region, the expression for the particle density function in terms of the real and imaginary parts of the generalized scattering amplitude varies according to θ angle due to different interference patterns between the scattered wave and the incident plane wave at different angles. In the forward, vertical, and backward scattering directions they are given as follows:

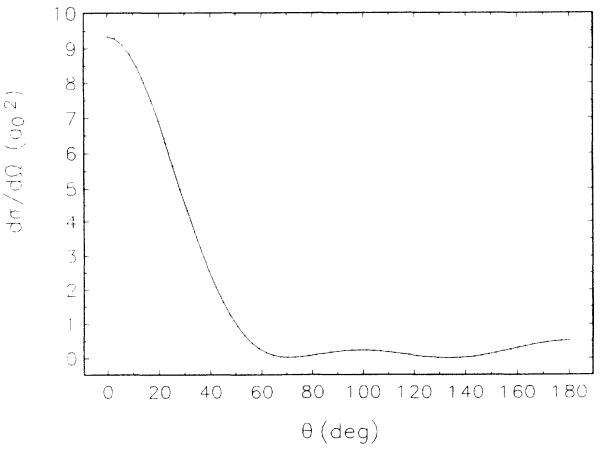

FIG. 8. Angular distribution of differential cross section. Square well potential scattering, $k_0=3.1$, $U=-10$. The scattering angle is denoted by θ.

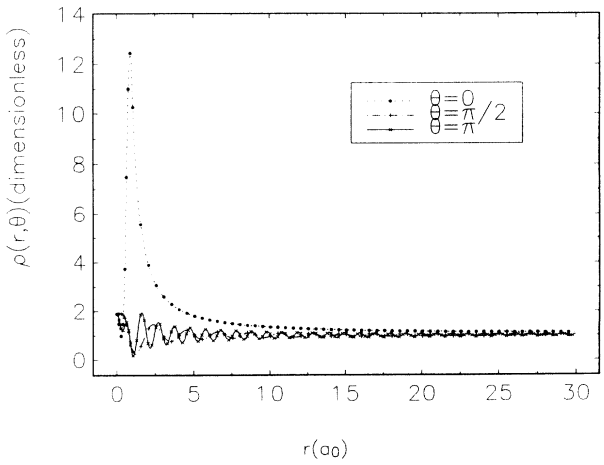

FIG. 9. Radial profiles of the particle density function $\rho(r,\theta)$. The radial distance r is in units of a_0, the atomic unit for length. Square well potential scattering, $k_0=3.1$, $U=-10$.

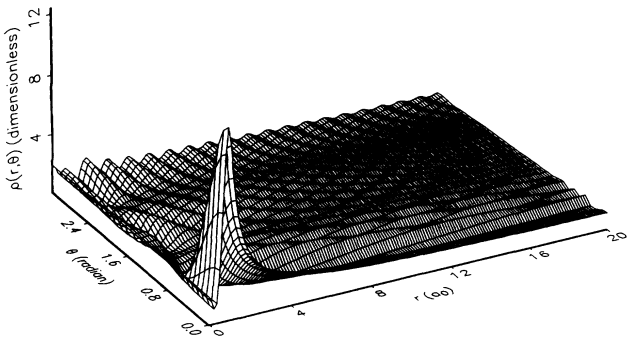

FIG. 10. Perspective 3D surface plot of the particle density function $\rho(r,\theta)$. Square well potential scattering, $k_0=3.1$, $U=-10$. The radial distance r is in units of a_0, the atomic unit for length. The scattering angle is denoted by θ.

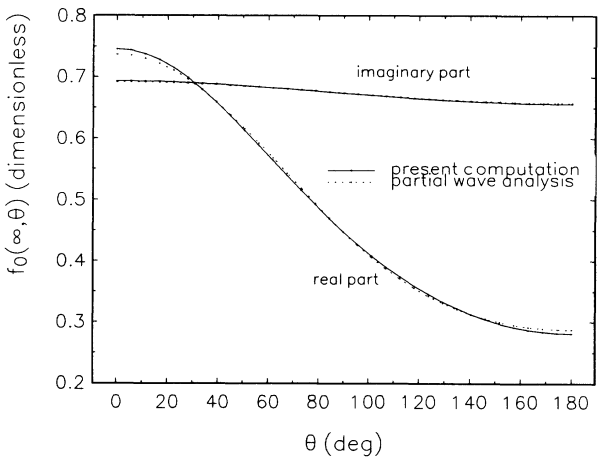

FIG. 11. Angular distribution of far-field scattering amplitude. (e^-,H) static field interaction potential scattering, $k_0=0.8$. The scattering angle is denoted by θ.

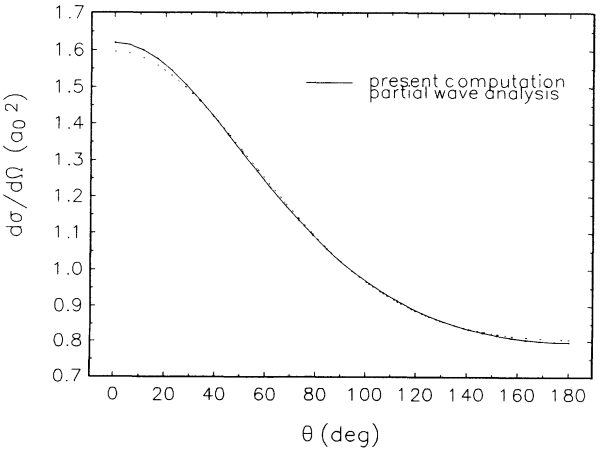

FIG. 12. Angular distribution of differential cross section. (e^-,H) static field interaction potential scattering, $k_0=0.8$. The scattering angle is denoted by θ.

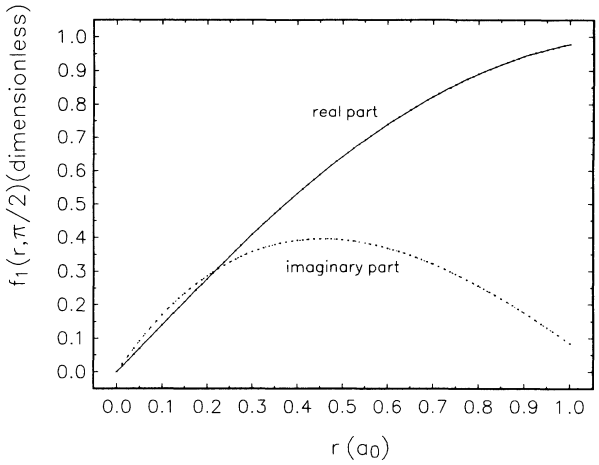

FIG. 13. Radial profiles of the generalized scattering amplitude $f_1(r,\theta)$ in the interior scattering region. (e^-,H) static field interaction potential scattering, $k_0=0.8$, $\theta=\pi/2$, vertical scattering direction. The radial distance r is in units of a_0, the atomic unit for length.

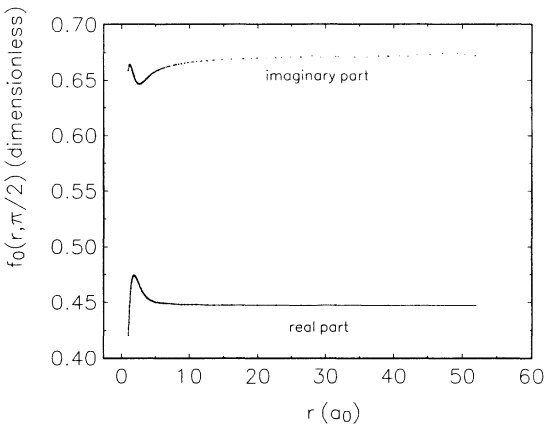

FIG. 14. Radial profiles of the generalized scattering amplitude $f_0(r,\theta)$ in the exterior scattering region. (e^-,H) static field interaction potential scattering, $k_0=0.8$, $\theta=\pi/2$, vertical scattering direction. The radial distance r is in units of a_0, the atomic unit for length.

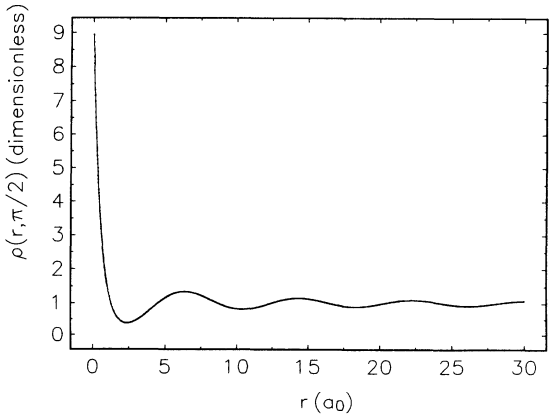

FIG. 15. Radial profile of the particle density function $\rho(r,\theta)$. (e^-,H) static field interaction potential scattering, $k_0=0.8$, $\theta=\pi/2$, vertical scattering direction. The radial distance r is in units of a_0, the atomic unit for length.

$$\rho(r,\theta)=\begin{cases}[1+\mathrm{Re}f_0/(k_0r)]^2+[\mathrm{Im}f_0]^2/(k_0r)^2 & \text{for } \theta=0 \quad (17)\\ 1+[(\mathrm{Re}f_0)^2+(\mathrm{Im}f_0)^2]/(k_0r)^2+2[\cos(k_0r)(\mathrm{Re}f_0)-\sin(k_0r)(\mathrm{Im}f_0)]/(k_0r) & \text{for } \theta=\pi/2 \quad (18)\\ 1+[(\mathrm{Re}f_0)^2+(\mathrm{Im}f_0)^2]/(k_0r)^2+2[\cos(2k_0r)(\mathrm{Re}f_0)-\sin(2k_0r)(\mathrm{Im}f_0)](k_0r) & \text{for } \theta=\pi. \quad (19)\end{cases}$$

Since the real and imaginary components of the generalized scattering amplitude in the exterior region are not radially oscillatory in any direction, it is readily seen that the forward direction is the only direction in which the particle density function is not oscillatory. The oscillation in the wave function and thus the particle density function, due to the interference between the plane wave and the scattered wave, increases from the forward direction to the backward direction (Fig. 10). Since the radial oscillation extends to the far field, this clearly explains the difficulty in methods which attempt to solve the wave function directly from the Schrödinger equation. In Ref. [15], the same pattern of radial profiles for the particle density function has been obtained for both a square well potential and a square barrier potential using the partial-wave analysis.

The present numerical method provides a global solution for a scattering problem. In addition to the all important far-field scattering amplitude and differential cross section, it provides detailed information regarding the scattering process in the near field. The generalized scattering amplitude can be used to reconstruct the global wave function from which relevant physical information can be extracted. As an example, it is interesting to note the sharp peak (Figs. 9 and 10) in the particle density function in the forward direction at $r=0.8875$, indicating a high concentration of particles during the scattering process at that location.

B. (e^-,H) static field potential scattering problem

The static field interaction between an electron and a ground state hydrogen atom is given by $U(r)=-2(1+1/r)\exp(-2r)$. Representative results for the scattering by this potential at $k_0=0.8$ are shown in Figs. 11–15. The boundary between the interior region and the exterior region is placed at $r=a=1$. Figures 11 and 12 show the close agreement between the generalized scattering amplitude solution and the partial-wave analysis for the far-field scattering amplitude and differential cross section. Three partial waves are included in the partial-wave analysis, with the phase shift values provided by Ref. [16]. The present computation uses the same radial grid as in the square well computation, but because of lower k_0 value, the angular grid is reduced to 33 grid points distributed uniformly in the angular range. The total cross section σ_t obtained from the integration of differential cross sections is equal to 13.557 while it is equal to 13.612 from the optical theorem. The three partial waves yield 13.577 for the total cross section.

The radial profiles of the generalized scattering amplitude and the particle density function in the vertical scattering direction are shown in Figs. 13–15. They exhibit similar behavior as those in the square well potential scattering. It is noted that Eqs. (17)–(19), based on Eq. (5), are valid for arbitrary potentials. Since the property of the generalized scattering amplitude, as dictated by the far-field condition, Eq. (8), is universal, the pattern exhibited by the particle density function is also universal in nature and it is independent of the form of the interaction potentials

V. CONCLUSION

The application of the generalized scattering amplitude to quantum potential scatterings has shown that, as in classical acoustic and electromagnetic scatterings, the generalized scattering amplitude is a fundamental quantity underlying the scattering process. It exhibits a behavior which is universal in nature, independent of the type of scatterings, the geometry of obstacles, and the form of interaction potentials. Specifically for quantum potential scatterings, the generalized scattering amplitude solution method is applicable to arbitrarily varying interaction potentials that vanish faster than the Coulomb potential in the far field. The theoretical formulation and numerical methods can be generalized and applied to three-dimensional scattering problems involving nonspherical interaction potentials, as demonstrated in the three-dimensional acoustic scattering problems [13]. Since complex atomic and molecular scattering processes often can be reduced to scatterings among composite scattering centers interacting via interatomic potentials or potential surfaces, the method described in this paper may be applied as a part of the overall theoretical and numerical method for complex scattering processes.

[1] E. C. Sullivan and A. Temkin, Comput. Phys. Commun. **25**, 97 (1982); **71**, 319 (1992).
[2] D. Neuhauser and M. Baer, J. Chem. Phys. **90**, 4351 (1989); T. Seidman and W. H. Miller, *ibid.* **97**, 2499 (1992).
[3] A. Bayliss and E. Turkel, J. Comput. Phys. **48**, 182 (1982); B. Enquist and A. Majda, Math. Comput. **31**, 629 (1977).
[4] R. T. Ling, AIAA J. **25**, 560 (1987); **26**, 151 (1988); **27**, 268 (1989).
[5] R. T. Ling, J. Appl. Phys. **64**, 3785 (1988).
[6] N. E. Logan, IEEE Proc. **63**, 773 (1965).
[7] E. Wolf, in *Coherence and Quantum Optics,* edited by L. Mandel and E. Wolf (Plenum, New York, 1973); M. Lax, Phys. Rev. **85**, 621 (1952).
[8] *Electromagnetic and Acoustic Scattering by Simple Shapes,* edited by J. J. Bowman, T. B. A. Senior, and P. L. E. Uslenghi (North-Holland, Amsterdam, 1969), pp. 5 and 6.

[9] A. Bayliss and E. Turkel, J. Comput. Phys. **49**, 443 (1983); C. C. Paige and M. A. Saunders, ACM Trans. Math. Software **8**, 195 (1982).
[10] Y. Saad and M. H. Schultz, Yale University Research Report No. DCS/RR 254, 1983 (unpublished).
[11] L. B. Wigton, N. J. Yu, and D. P. Young (unpublished).
[12] R. T. Ling, Comput. Phys. Commun. **68**, 213 (1991).
[13] R. T. Ling, in *Proceedings of the First International Conference on Theoretical and Computational Acoustics,* edited by D. Lee (World Scientific, Singapore, in press).
[14] M. Inokuti, Comments At. Mol. Phys. **10**, 99 (1981); D. W. Norcross, in *Atoms in Astrophysics,* edited by P. G. Burke *et al.* (Plenum, New York, 1983).
[15] S. Brandt and H. D. Dahmen, *The Picture Book of Quantum Mechanics* (Wiley, New York, 1985), pp. 242 and 264.
[16] B. H. Bransden, *Atomic Collision Theory* (Benjamin, New York, 1970), p. 17.